# Titanium based materials / Combinations of metallic biomaterials / Special Materials

## 8.5. Titanium based materials

### 8.5.1. Groups of alloys

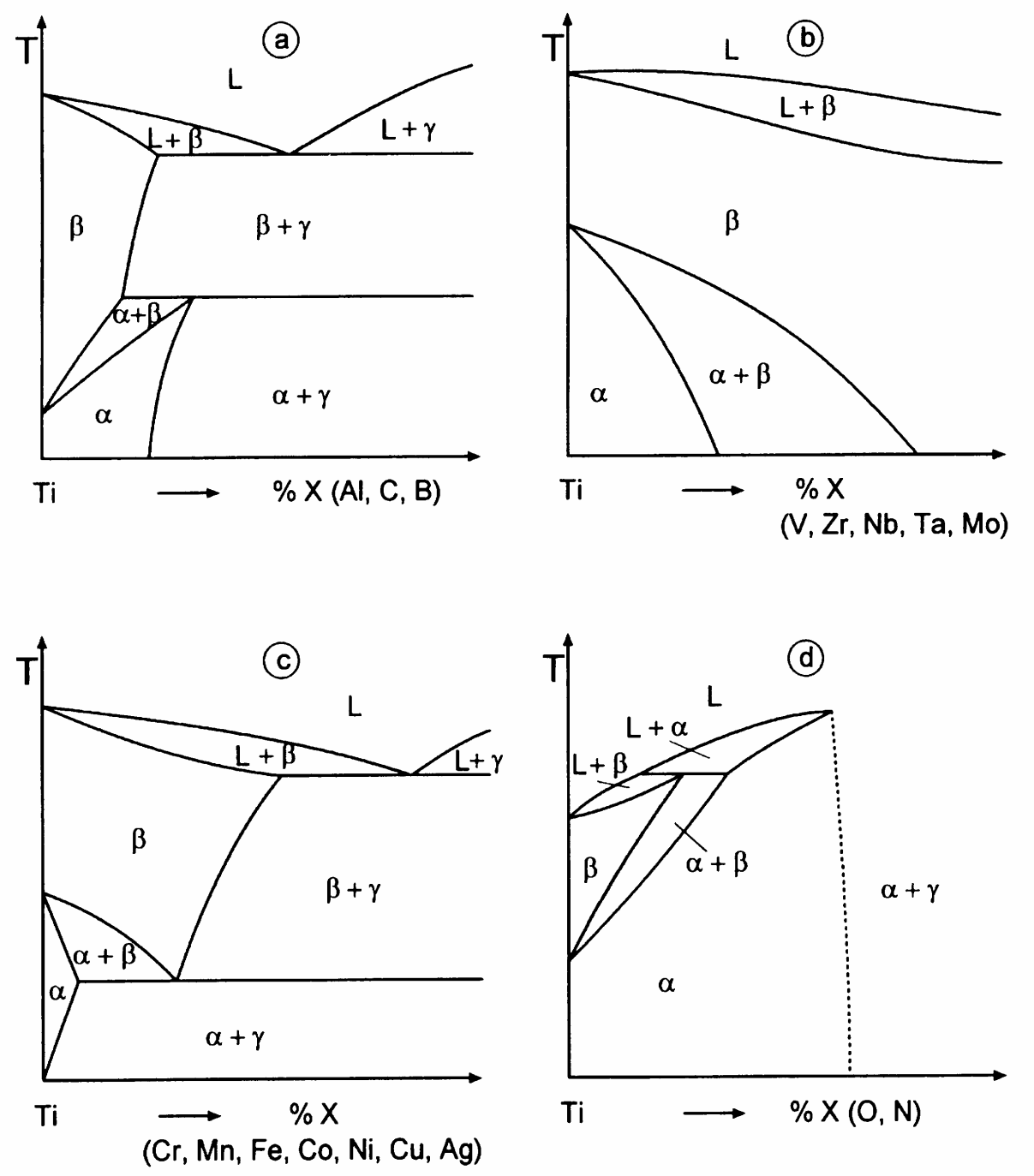


α-alloys (hexagonal Closed packed) ..... β-alloys (body Centered Cubic)

# Effects of alloying elements on titanium alloy structure

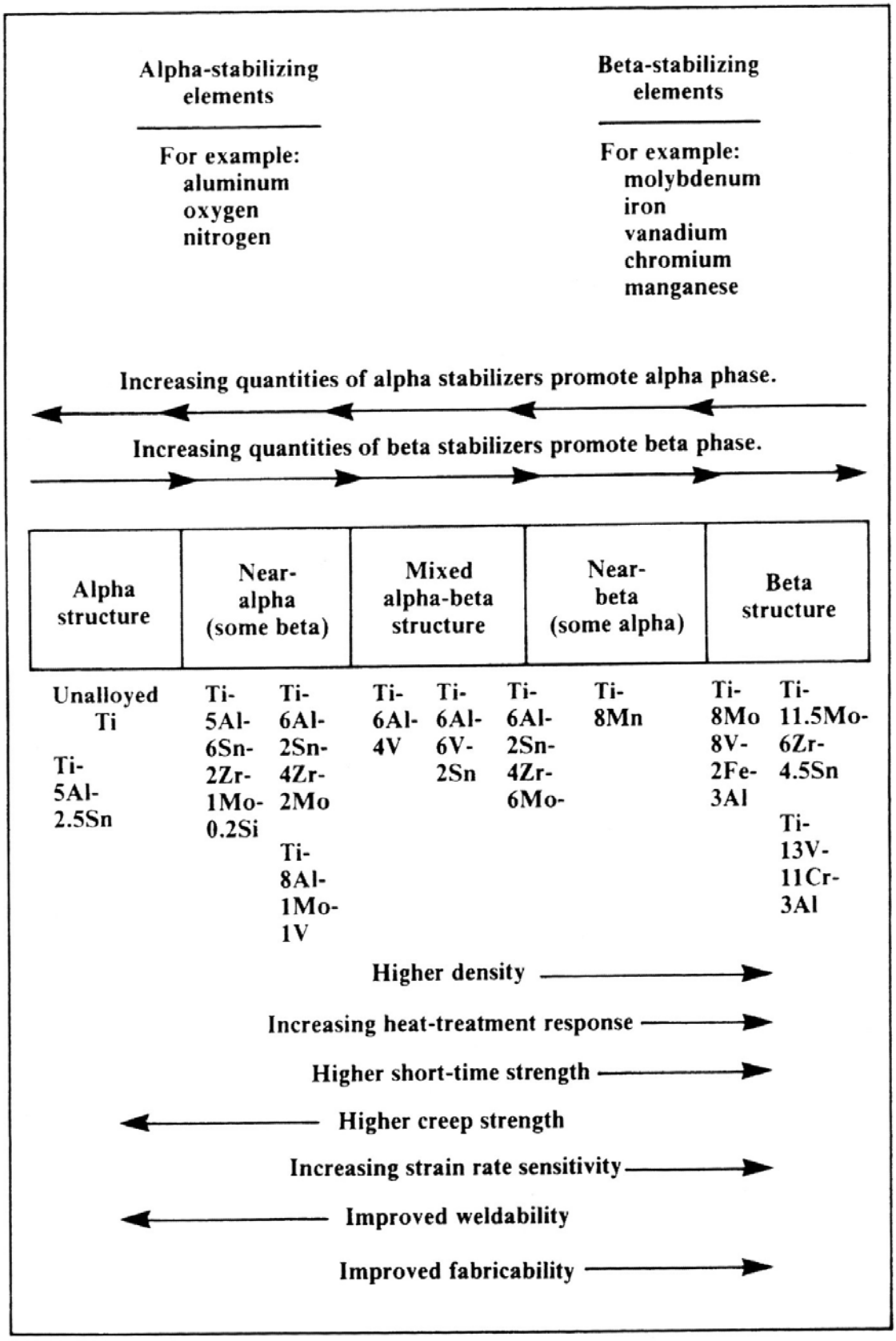


**Fig. 3.5.** Effects of alloying elements on titanium alloy structure. (Reproduced by permission of ASM International, Metals Park OH, USA).

# Chemical compositions of titanium alloys

**Table 3.1.** Chemical composition and standards for selected titanium biomaterials.

| Grade Name and Type | UNS Number | ASTM Standard | ISO Standard | Chemical Composition Nominal Weight % |
|---|---|---|---|---|
| Ti CP-1 (Alpha) | R50250 | ASTM F 67 | ISO 5832-2 | **C** 0.10 max **Fe** 0.20 max **H** 0.015 max **N** 0.03 max **O** 0.18 max **Ti** rem |
| Ti CP-2 (Alpha) | R50400 | ASTM F 67 | ISO 5832-2 | **C** 0.10 max **Fe** 0.30 max **H** 0.015 max **N** 0.03 max **O** 0.25 max **Ti** rem |
| Ti CP-3 (Alpha) | R50550 | ASTM F 67 | ISO 5832-2 | **C** 0.10 max **Fe** 0.30 max **H** 0.015 max **N** 0.05 max **O** 0.35 max **Ti** rem |
| Ti CP-4 (Alpha) | R50700 | ASTM F 67 | ISO 5832-2 | **C** 0.10 max **Fe** 0.50 max **H** 0.015 max **N** 0.05 max **O** 0.40 max **Ti** rem |
| Ti-3Al-2.5V (Alpha/Beta) | R56320 | ASTM B 348 F-04.12.06 | --- | **Al** 3.0 **C** 0.05 max **Fe** 0.13 **H** 0.015 max **N** 0.01 **O** 0.10 **Ti** rem **V** 2.5 |
| Ti-5Al-2.5Fe (Alpha/Beta) | --- | | ISO 5832-10 | **Al** 5.0 **C** 0.05 max **Fe** 2.5 **H** 0.015 max **N** 0.05 max **O** 0.25 **Ti** rem |
| Ti-6Al-4V (Alpha/Beta) | R56400 | ASTM F 1472 | ISO 5832-3 | **Al** 6.0 **C** 0.10 max **Fe** 0.20 **H** 0.015 max **N** 0.03 **O** 0.20 max **Ti** rem **V** 4.0 |
| Ti-6Al-4V ELI (Alpha/Beta) | R56401 | ASTM F 136 | ISO 5832-3 | **Al** 6.0 **C** 0.10 max **Fe** 0.20 **H** 0.015 max **N** 0.03 **O** 0.13 max **Ti** rem **V** 4.0 |
| Ti-6Al-7Nb (Alpha/Beta) | R56700 | ASTM F 1295 | ISO 5832-11 | **Al** 6.0 **C** 0.08 max **Fe** 0.15 **H** 0.009 max **Nb** 7.0 **N** 0.03 **O** 0.20 max **Ta** 0.5 max **Ti** rem |
| Ti-15Mo (Beta) | R58150 | ASTM F 2066 | --- | **C** 0.05 max **Fe** 0.1 **H** 0.015 max **Mo** 15.0 **N** 0.01 **O** 0.15 **Ti** rem |
| Ti-13Nb-13Zr (Beta) | R58130 | ASTM F 1713 | --- | **C** 0.08 max **Fe** 0.1 **H** 0.02 max **Nb** 13.0 **N** 0.01 **O** 0.1 **Ti** rem **Zr** 13.0 |
| Ti-16Nb-10Hf (Beta) | --- | --- | --- | **C** 0.05 max **Fe** 0.05 **H** 0.015 max **Hf** 9.5 **Nb** 16.0 **N** 0.002 **O** 0.1 **Ti** rem |
| Ti-15Mo-2.8Nb-0.2Si (Beta) | --- | --- | --- | **C** 0.02 max **Fe** 0.2 **H** 0.02 max **Mo** 15.0 **N** 0.01 **O** 0.18 **Ti** rem **Nb** 2.8 **Si** 0.2 |
| Ti-12Mo-6Zr-2Fe (Beta) | R58120 | ASTM F 1813 | --- | **C** 0.02 max **Fe** 2.0 **H** 0.02 max **Mo** 12.0 **N** 0.01 **O** 0.18 **Ti** rem **Zr** 6.0 |
| Ti-12Mo-5Zr-5Sn (Beta) | --- | --- | --- | **C** 0.02 max **Fe** 0.2 **H** 0.02 max **Mo** 12.0 **N** 0.01 **O** 0.18 **Ti** rem **Zr** 5.0 **Sn** 5.0 |
| Ti-15Mo-5Zr-3Al (Beta) | --- | --- | --- | **Al** 3.0 **C** 0.02 max **Fe** 0.2 **H** 0.02 max **Mo** 15.0 **N** 0.01 **O** 0.18 **Ti** rem **Zr** 5.0 |
| Ti-30Ta (Beta) | --- | --- | --- | **C** 0.05 max **Fe** 0.1 **H** 0.015 max **N** 0.01 **O** 0.15 **Ti** rem **Ta** 30.0 |
| Ti-45Nb (Beta) | R58450 | AMS 4982 | --- | **C** 0.04 max **Fe** 0.1 **H** 0.003 max **Nb** 45.5 **N** 0.01 **O** 0.1 **Ti** rem |
| Ti-35Zr-10Nb (Beta) | --- | --- | --- | **C** 0.05 max **Fe** 0.05 **H** 0.015 max **Nb** 10.5 **N** 0.002 **O** 0.1 **Ti** rem **Zr** 35.2 |
| Ti-35Nb-7Zr-5Ta (Beta) | R58350 | Task Force F-04.12.23 | --- | **C** 0.05 max **Fe** 0.05 **H** 0.015 max **Nb** 35.5 **N** 0.02 **O** 0.15 **Ta** 5.7 **Ti** rem **Zr** 7.3 |
| Ti-55.8Ni (Intermetallic) | --- | ASTM F 2063 | --- | **C** 0.05 max **Fe** 0.02 **H** 0.003 max **Ni** 55.8 **N** 0.01 **O** 0.05 **Ti** rem |

# Mechanical properties of selected titanium alloys

**Table 3.2.** Mechanical properties of selected titanium biomaterials.

| Grade Designation and Type | Metallurgical Condition (footnote) | Tensile Strength ksi. (MPa) | 0.2% Yield Strength ksi. (MPa) | Elon-gation % | Reduction in Area % | Typical Hardness (Rockwell) |
|---|---|---|---|---|---|---|
| Ti CP-1 (Alpha) | 1,300 °F anneal (a) | 35 (241) | 25 (172) | 24 | 30 | 70 HRB |
| Ti CP-2 (Alpha) | 1,300 °F anneal (a) | 50 (345) | 40 (276) | 20 | 30 | 80 HRB |
| Ti CP-3 (Alpha) | 1,300 °F anneal (a) | 65 (448) | 55 (379) | 18 | 30 | 90 HRB |
| Ti CP-4 (Alpha) | 1,300 °F anneal (a) | 80 (552) | 70 (483) | 15 | 25 | 100 HRB |
| Ti-3Al-2.5V (Alpha/Beta) | 1,300 °F anneal (a) | 100 (690) | 85 (586) | 15 | 25 | 24 HRC |
| Ti-5Al-2.5Fe (Alpha/Beta) | --- | --- | --- | --- | --- | --- |
| Ti-6Al-4V (Alpha/Beta) | 1,300 °F anneal (a) | 135 (931) | 125 (862) | 15 | 30 | 36 HRC |
| Ti-6Al-4V ELI (Alpha/Beta) | 1,725 °F anneal (b) | 125 (862) | 115 (793) | 10 | 25 | 32 HRC |
| Ti-6Al-7Nb (Alpha/Beta) | 1,300 °F anneal (a) | 125 (862) | 115 (793) | 10 | 25 | 32 HRC |
| Ti-15Mo (Beta) | 1,475 °F anneal (c) | 115 (793) | 95 (655) | 22 | 60 | 24 HRC |
| Ti-13Nb-13Zr (Beta) | Capability aged | 125 (860) | 105 (725) | 8 | 15 | --- |
| Ti-16Nb-10Hf (Beta) | 1,560 °F + water quench (d) | 85 (486) | 40 (276) | 16 | --- | --- |
| Ti-15Mo-2.8Nb-0.2Si (Beta) | 1,475 °F anneal (c) | 115 (793) | 95 (655) | 22 | 60 | 24 HRC |
| Ti-12Mo-6Zr-2Fe (Beta) | 1,400 °F anneal (e) | 145 (1,000) | 140 (965) | 15 | 40 | 33 HRC |
| Ti-12Mo-5Zr-5Sn (Beta) | --- | --- | --- | --- | --- | --- |
| Ti-15Mo-5Zr-3Al (Beta) | --- | --- | --- | --- | --- | --- |
| Ti-30Ta (Beta) | --- | --- | --- | --- | --- | --- |
| Ti-45Nb (Beta) | As drawn wire | 70 (483) | 65 (448) | 12 | 55 | --- |
| Ti-35Zr-10Nb (Beta) | Hot Rolled | 130 (897) | 90 (621) | 16 | --- | --- |
| Ti-35Nb-7Zr-5Ta (Beta) | 1,300 °F anneal (a) | 120 (827) | 115 (793) | 20 | 55 | 35 HRC |
| Ti-55.8Ni (Intermetallic) | 1,475 °F anneal (c) | 150 (1,034) | 50 (345) | 20 | --- | --- |

*HRB* = Hardness, Rockwell B Scale. *HRC* = Hardness, Rockwell C Scale.
a: approx. 700 °C b: approx. 940 °C c: approx. 800 °C d: approx. 850 °C e: approx. 760 °C.

# pure α-structure

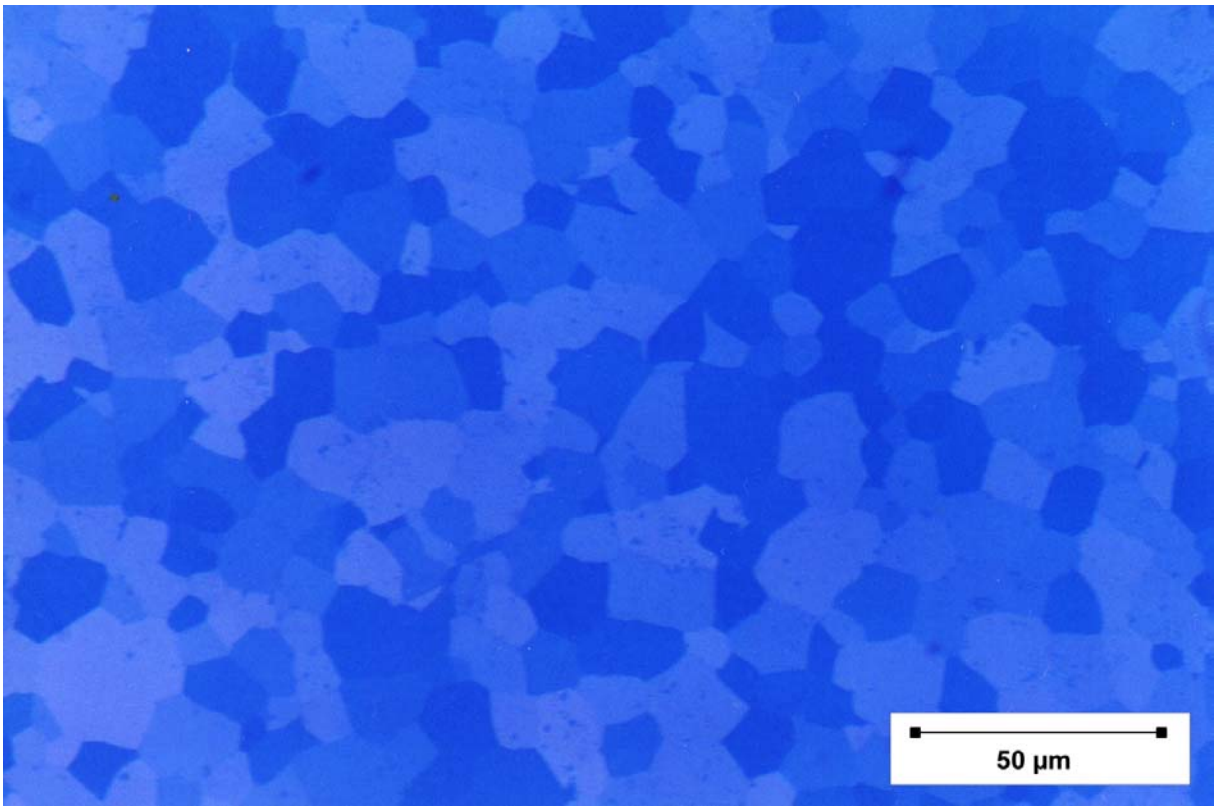


Ti, CP-1 ; average grain size = 10.8 ± 5.6 µm

# Mixed α-β-structure

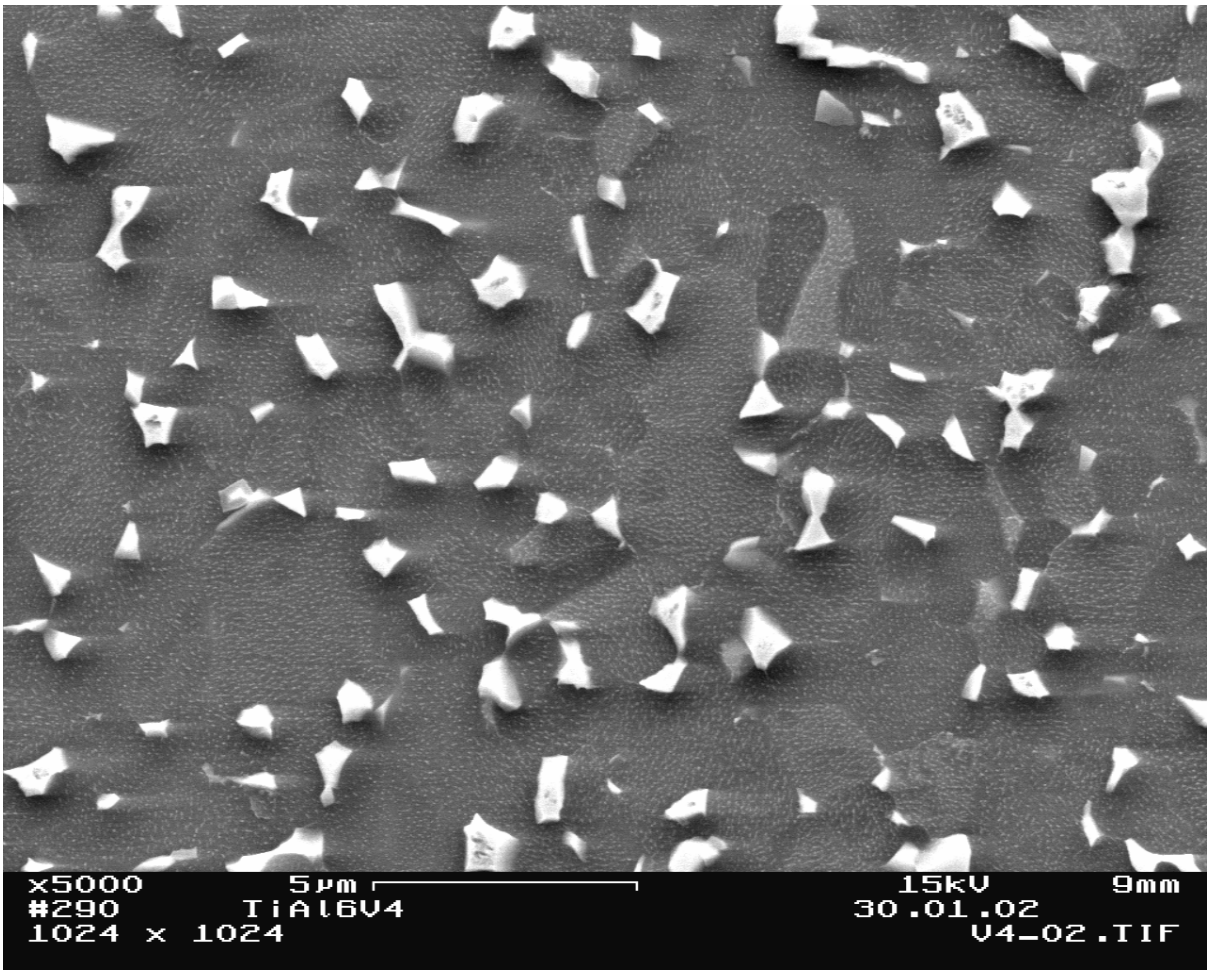


Ti6Al4V ; average grain size = 1.9 ± 0.6 µm
Dark = α ; bright = β (20 – 25 mass% V)

# Mixed α-β-structure

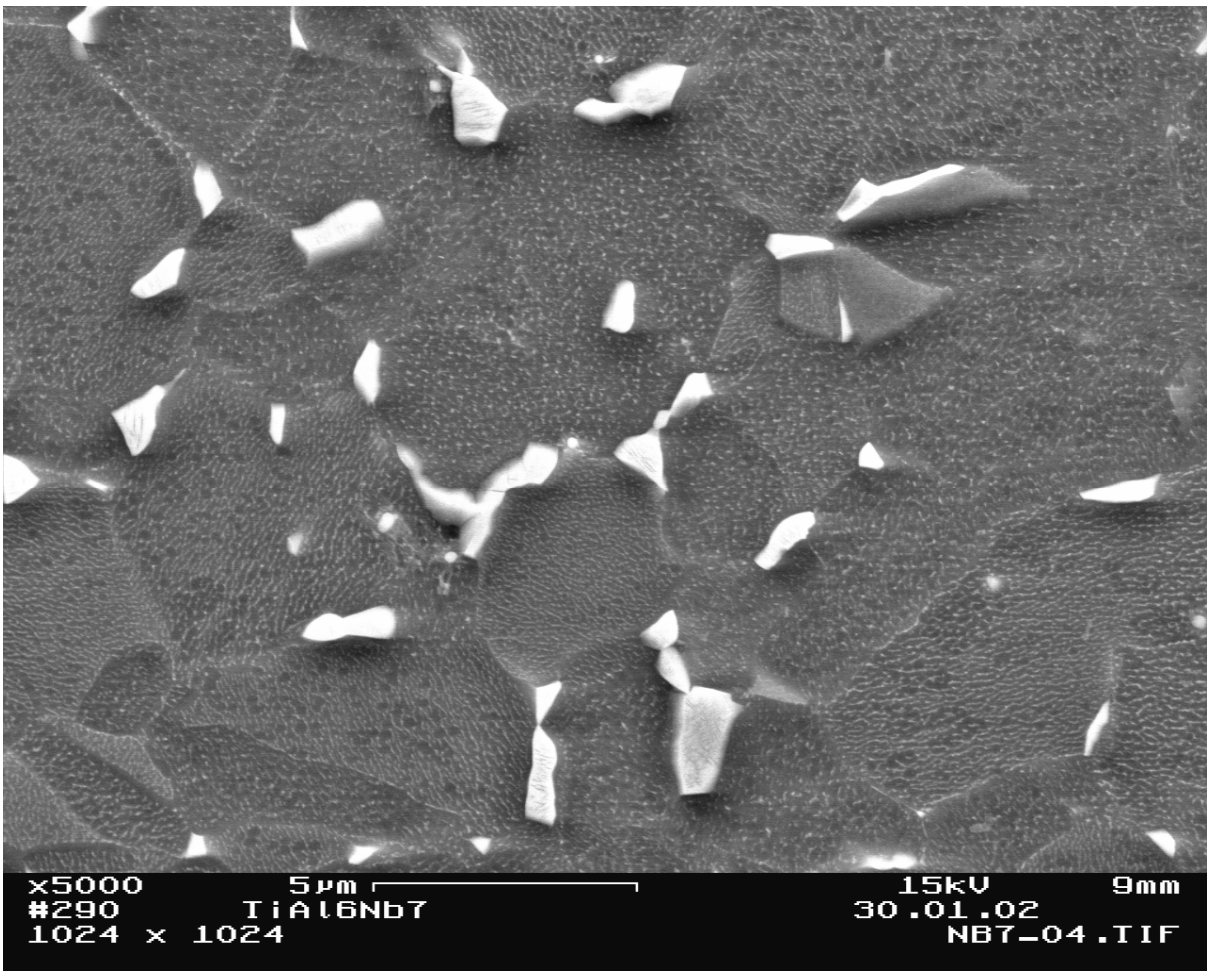


Ti6Al7Nb ; average grain size = 3.2 ± 0.6 µm
Dark = α ; bright = β (18 – 21 mass% Nb)

# Lateral distribution of alloying elements in Ti6Al7Nb

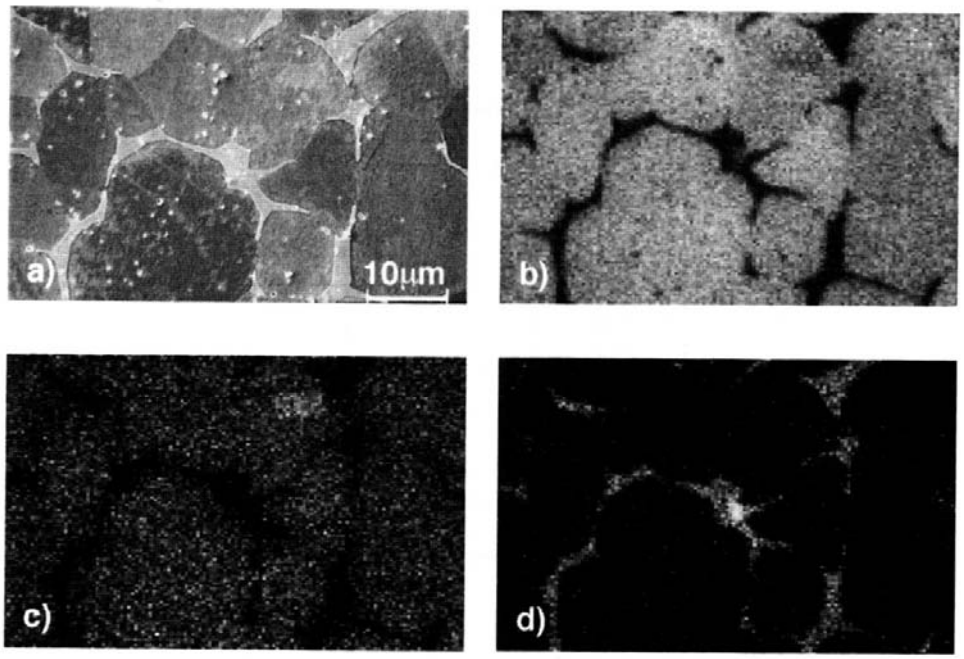


**Fig. 7.17.** Scanning Auger microscopy (SAM) images of the native oxide film on Ti–6Al–7Nb with artificially coarsened metal microstructure (to make imaging analysis easier): **a.** secondary electron image of the analyzed area; **b.** SAM map of Ti; **c.** Al; **d.** Nb [74]. (Reproduced from [74] by permission of Kluwer Publishers).

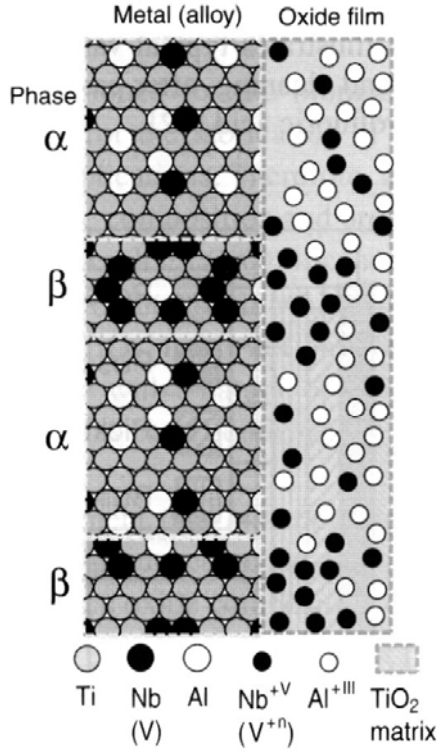


**Fig. 7.15.** Schematic representation (in cross-section) of a native oxide film on a heterogeneous alloy TiAlV or TiAlNb (for details: see text).

# Influence of surface treatments on chemical surface composition

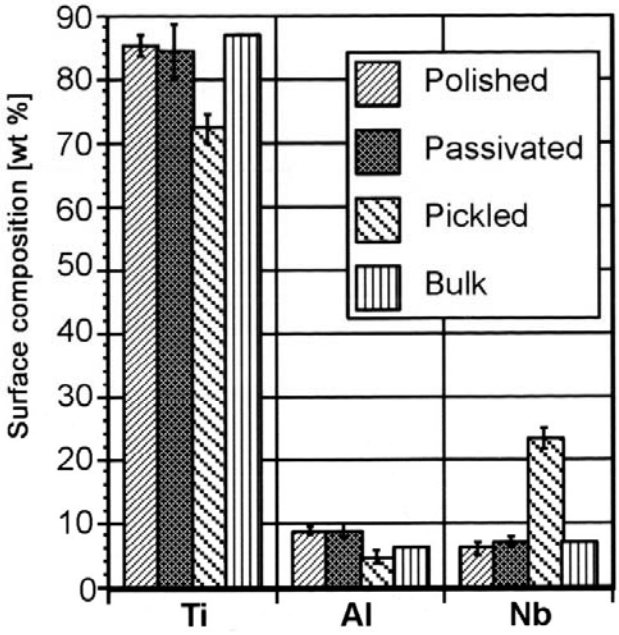


**Fig. 7.16.** Composition of the oxide film at the surface of alloy Ti–6Al–7Nb (XPS data converted to weight percent, normalized to Ti + Al + Nb = 100 wt%) compared with the bulk composition. The three different surfaces are mechanically polished and cleaned, passivated in nitric acid, and pickled in nitric acid/hydrofluoric acid respectively [74]. (Reproduced from [74] by permission of Kluwer Publishers).

# Depth distribution of alloying elements in anodic oxide layers on Ti6Al4V

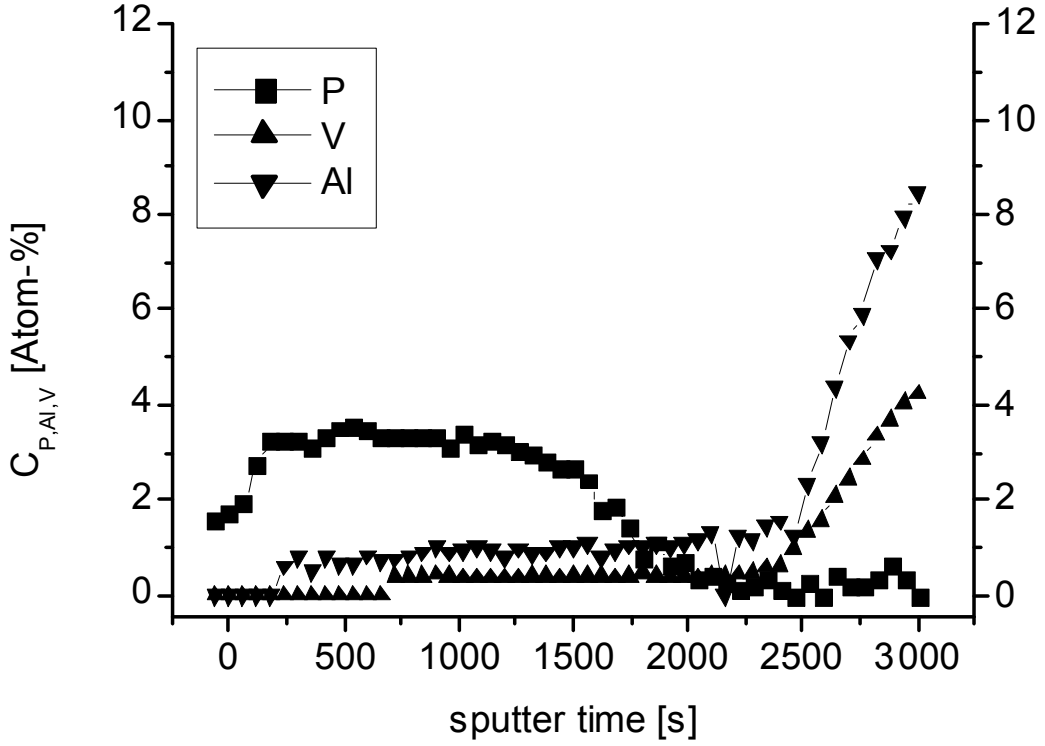


gs, Ti6Al4V; 6.37 mA $cm^{-2}$, 80 V

$d_{eff}$ = 160 – 180 nm

# Depth distribution of alloying elements in anodic oxide layers on Ti6Al7Nb

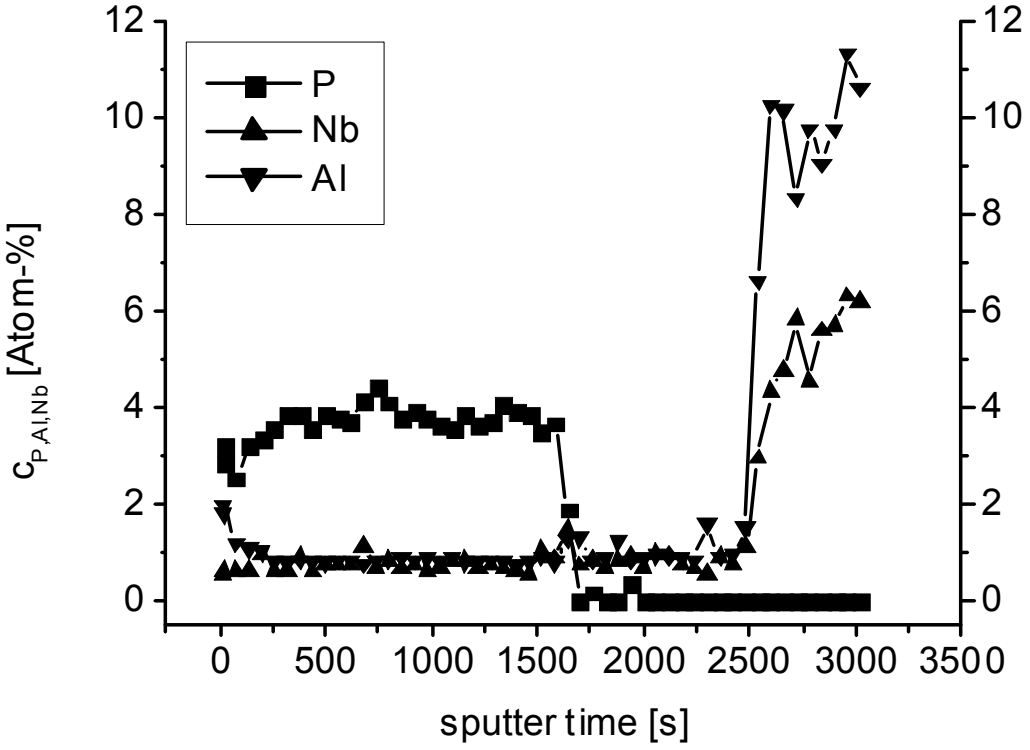


gs, Ti6Al7Nb; 6.37 mA $cm^{-2}$, 80 V
$d_{eff}$ = 160 – 180 nm

# properties of oxide layers

conduction mechanism - electronic
n-type semiconducting
ionic

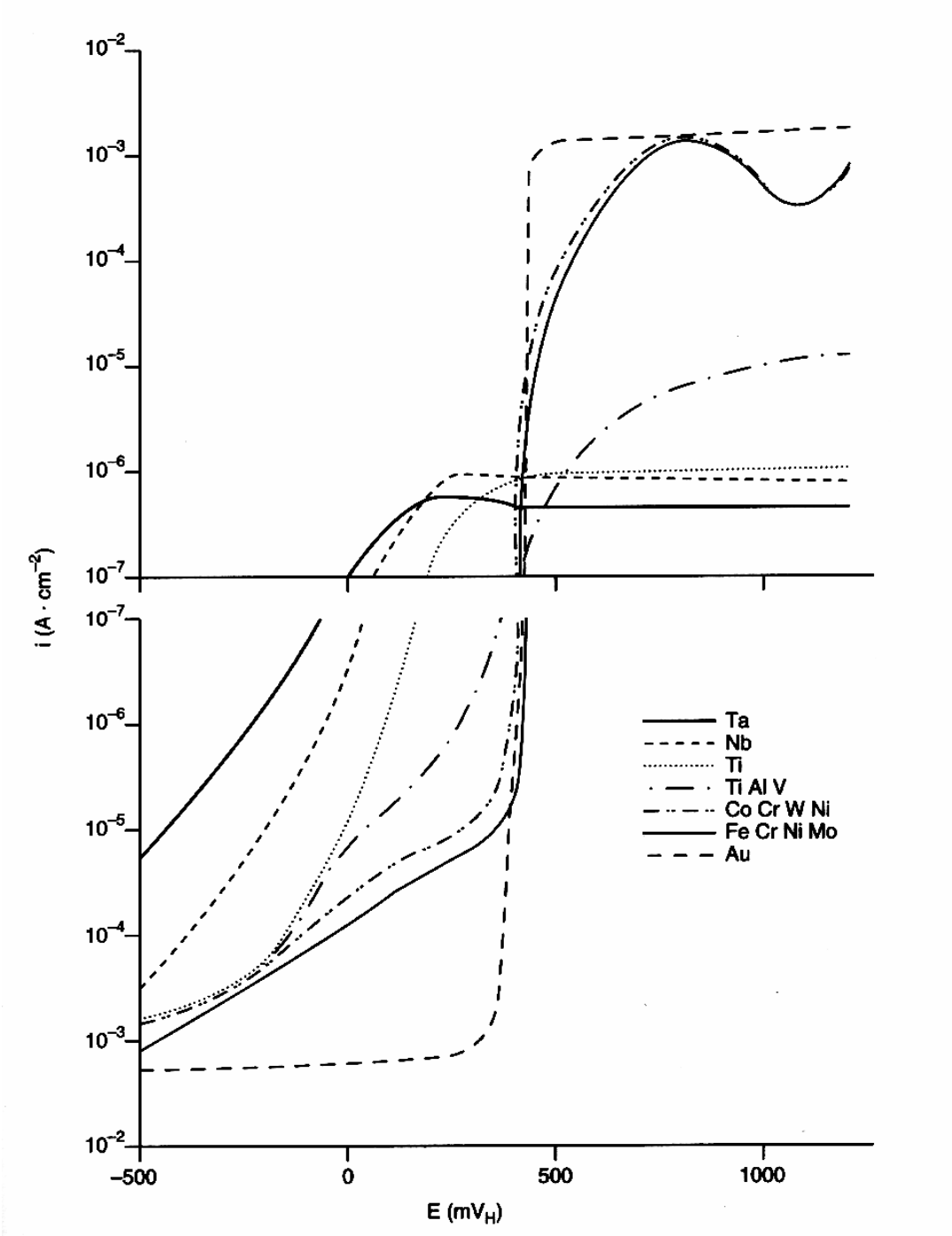

# Oxide layers on titanium based alloys

n-type semiconductors

Characterized by flatband potential $U_{FB}$ and donor density $N_d$

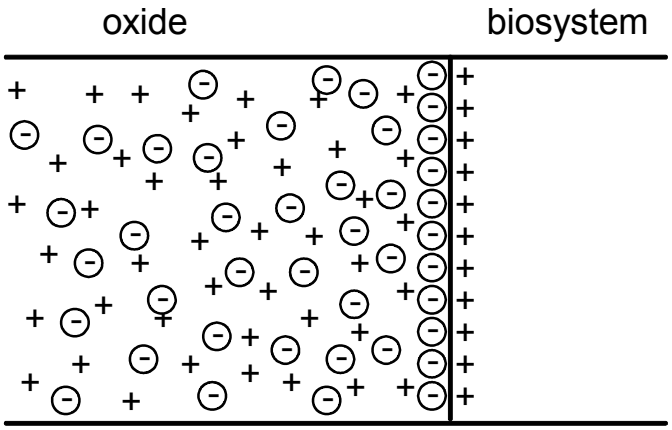


$U = U_{redox} < U_{FB}$; $I_{redox}$ unimpeded

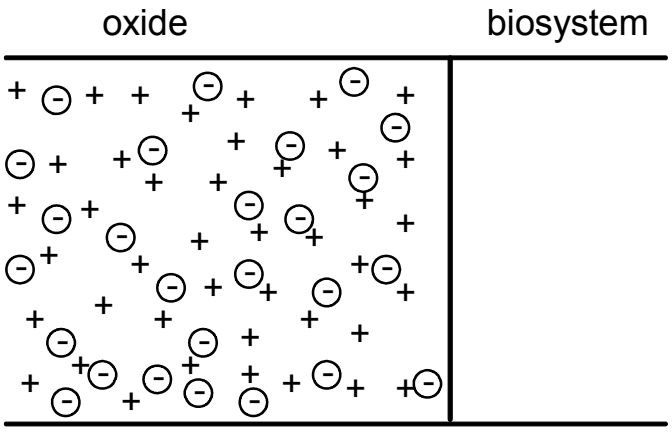


$U = U_{redox} \approx U_{FB}$; $I_{redox} = f(U, N_d)$

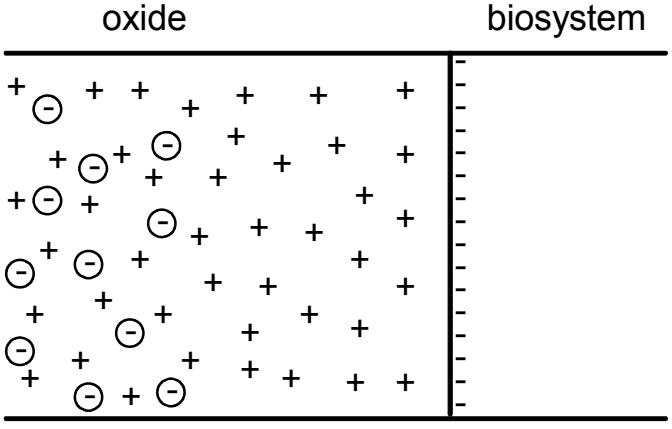


$U = U_{redox} > U_{FB}$; $I_{redox} = f(N_d)$

# Mott-Schottky-Equation

$$\frac{1}{C_{sc}^2} = \frac{2}{q\varepsilon\varepsilon_0 N_d}\left(U - U_{FB} - \frac{kT}{q}\right) \approx \frac{1}{C^2}$$

with

C ... capacity
$C_{SC}$ ... capacity of space charge layer in the n-type semiconductor
q ... charge of electron ($1.602 \cdot 10^{-19}$ As)

**$N_d$ ... donor density (in n-type semiconductor)**

$\varepsilon_0$ ... absolute dielectric constant ($8.86 \cdot 10^{-14}$ F $cm^{-1)}$
$\varepsilon$ ... relative dielectric constant

**$U_{FB}$… flatband potential**

k ... Boltzmann constant ($1.38 \cdot 10^{-23}$ Ws $K^{-1}$)
so with kT/q = 26 mV

# Typical Mott-Schottky-Plots

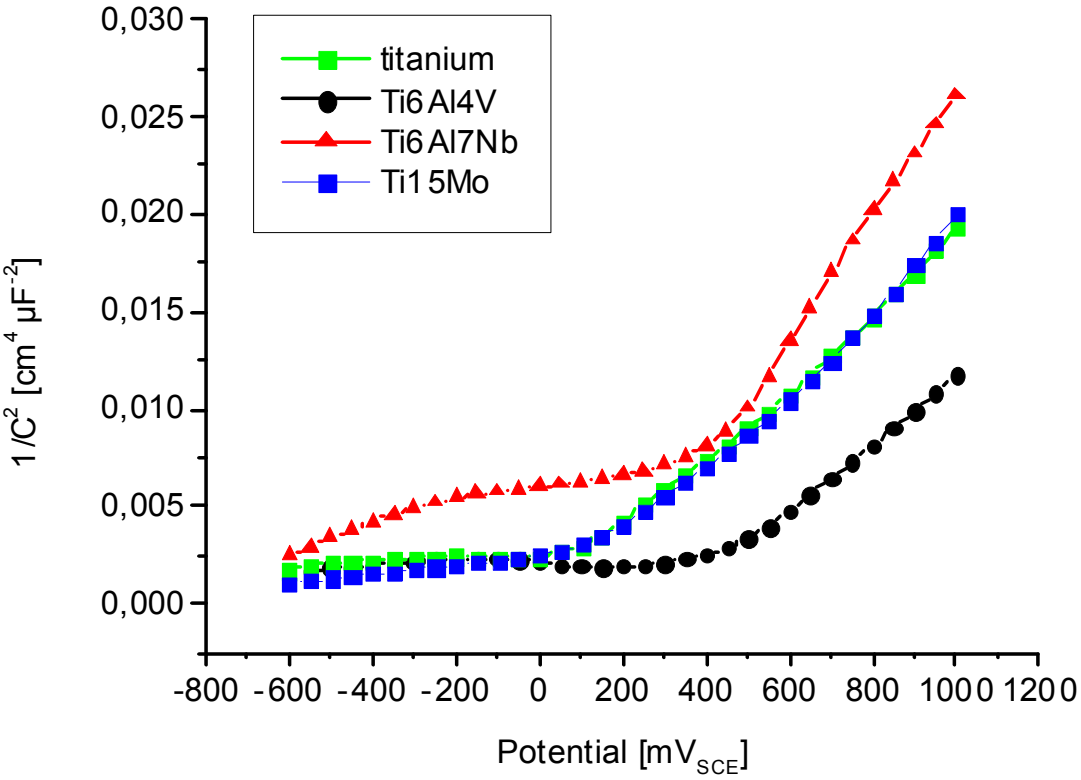


0.133 M Phosphate buffer solution, pH =7.4

typical redox potentials in biological systems 350 – 550 $mV_{SCE}$
(D. Velten et al., J. Biomed. Mater. Res. **59** (2002) 18.)

# Flatband potentials of different materials as f (pH)

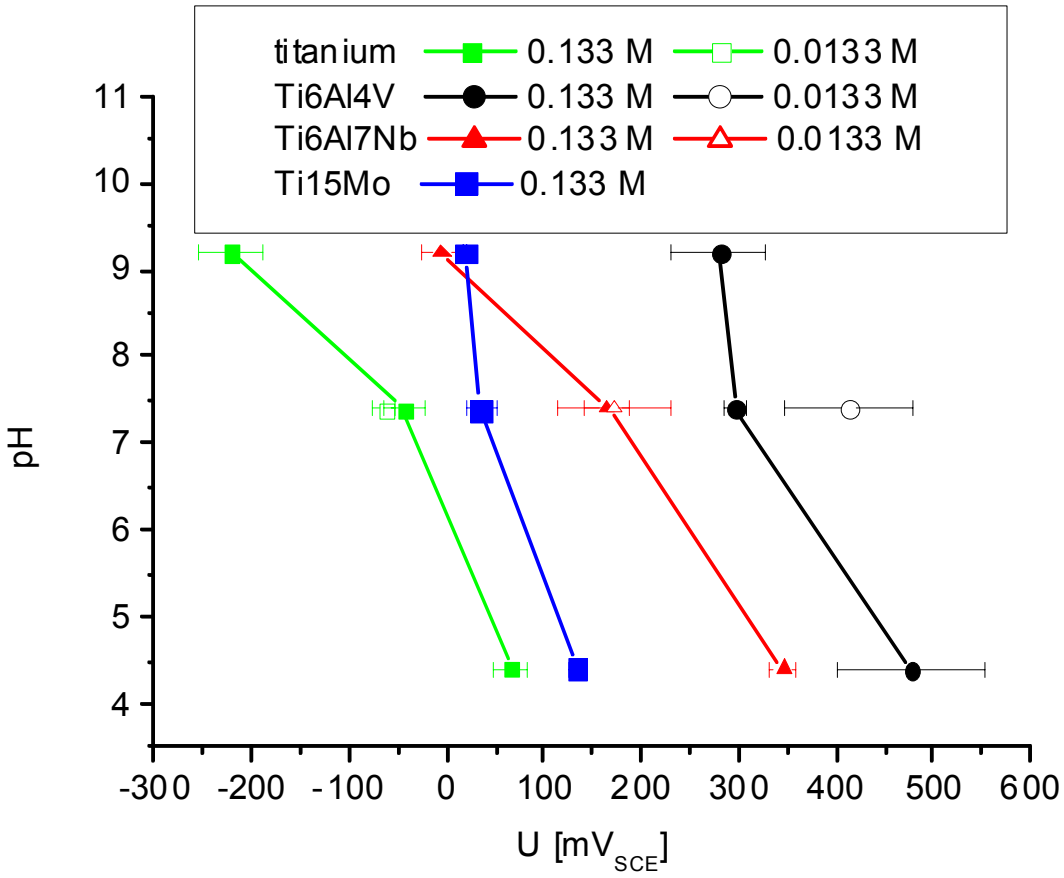

# Donor densities of different materials as f (pH)

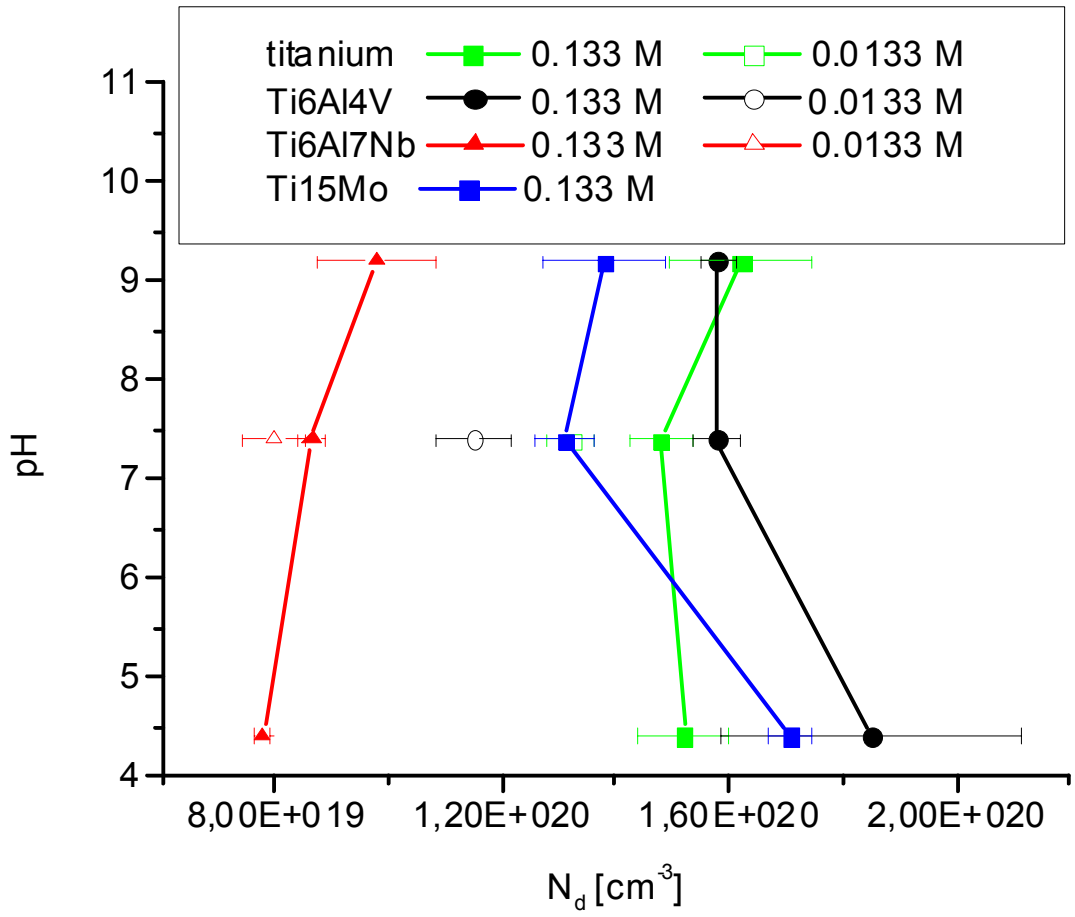

# Charge density-potential curves for galvanostatic polarization of different titanium alloys

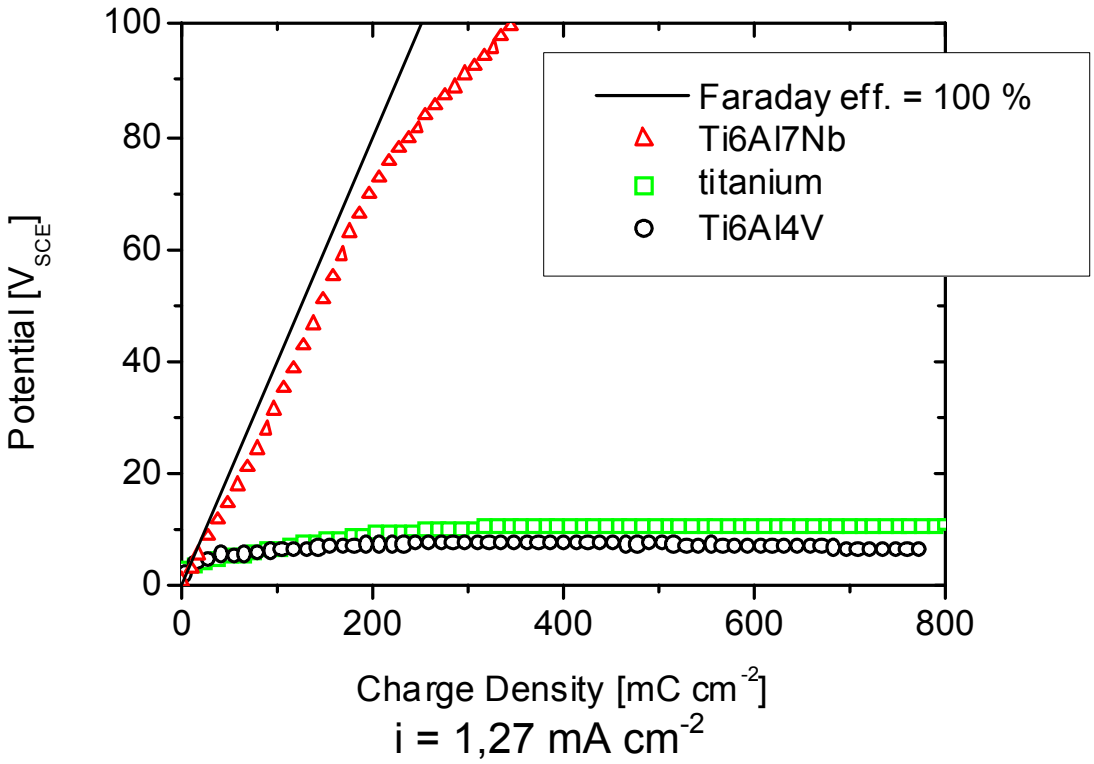


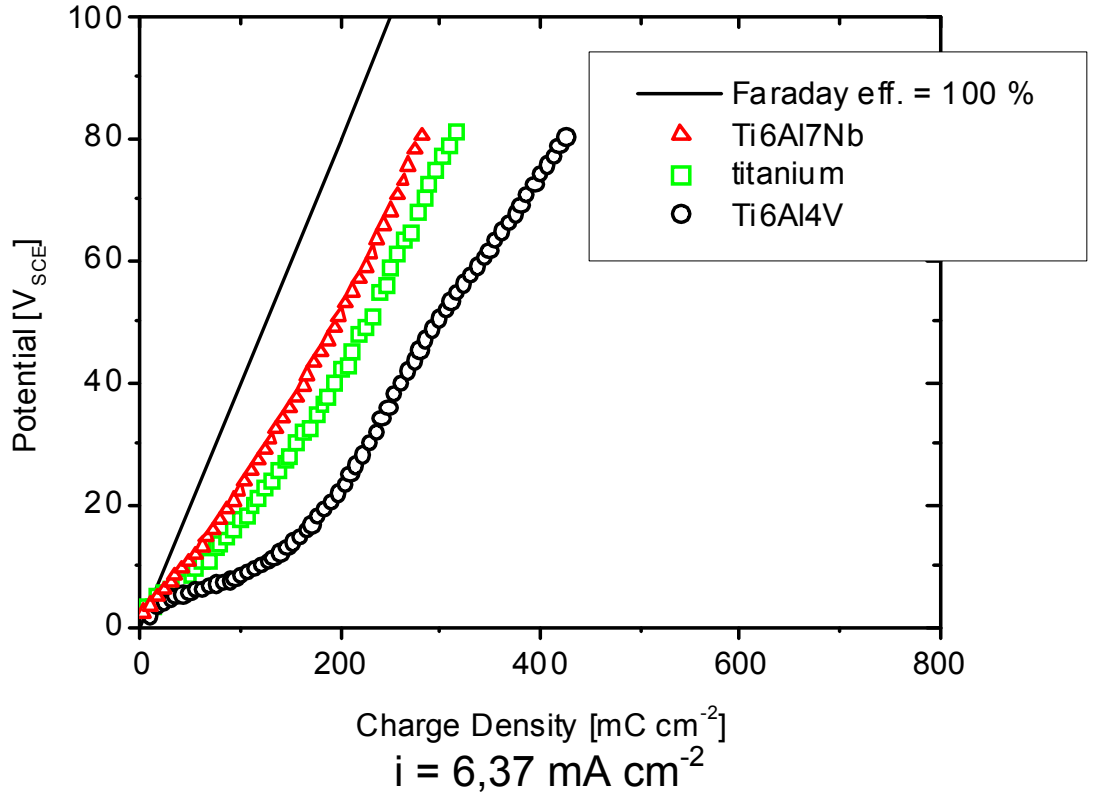

# Morphology of anodic oxide layers

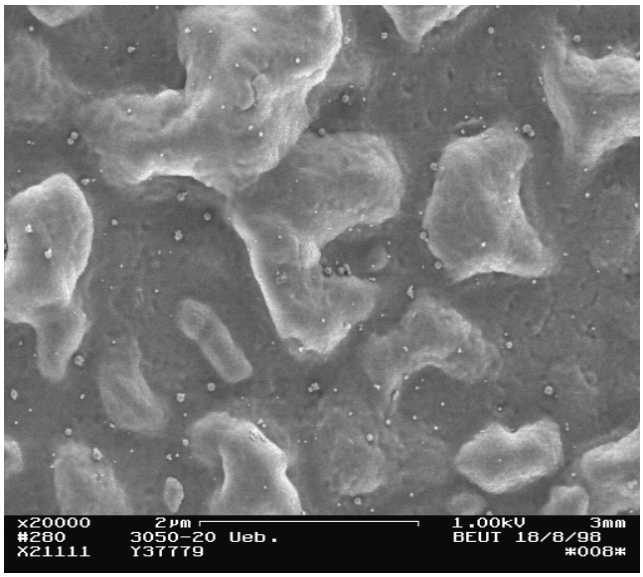


**Titanium**

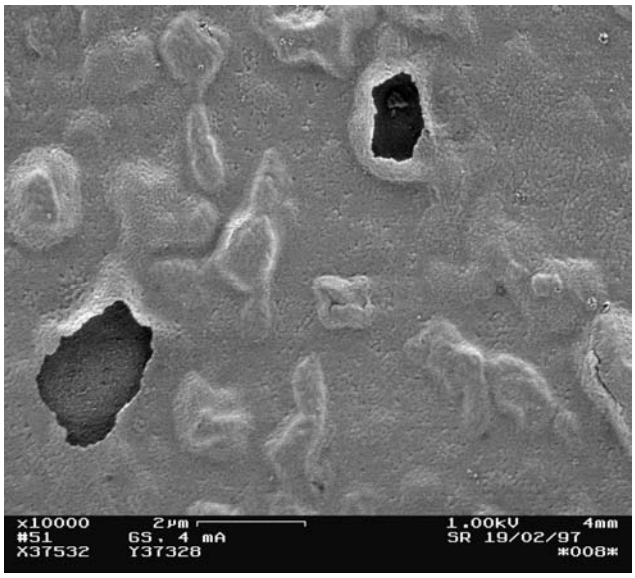


**Ti6Al4V**

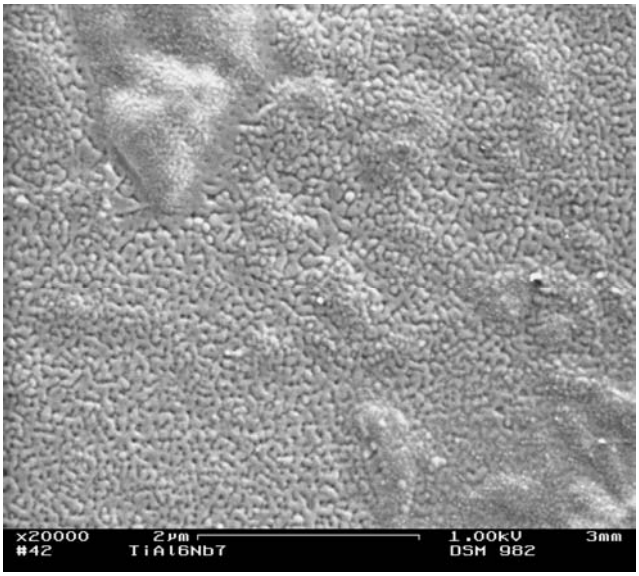


**Ti6Al7Nb**

# Chemical / electrochemical processes

oxide formation in PB oxide/electrolyte

$Ti^{4+} + 3\ H_2O \rightarrow TiO^{2+} + 2\ H_3O^+$

$TiO^{2+} + 4\ H_2O \rightarrow TiO(OH)_2 + 2\ H_3O^+$

$TiO(OH)_2 \rightarrow TiO_{2-x}(OH)_{2x} + (1-x)\ H_2O$

$\mathbf{(TiO_{1-x}(OH)_{2x+1})^+} \Leftrightarrow$

$(H^+ +)\ TiO_{2-x}(OH)_{2x}\ (+\ HO^-) \Leftrightarrow$

$\mathbf{(TiO_{3-x}(OH)_{2x-1})^-} + H_2O$

oxide formation in PB metal/oxide

$6\ H_2O \rightarrow 2\ O^{2-} + 4\ H_3O^+$

**parallel reaction(s)**

**oxygen evolution**

$\mathbf{6\ H_2O \rightarrow O_2 + 4\ H_3O^+ + 4\ e^-}$

$\mathbf{BM \rightarrow BM^+ + e^-}$

**redox reactions with adsorbed biomolecules**

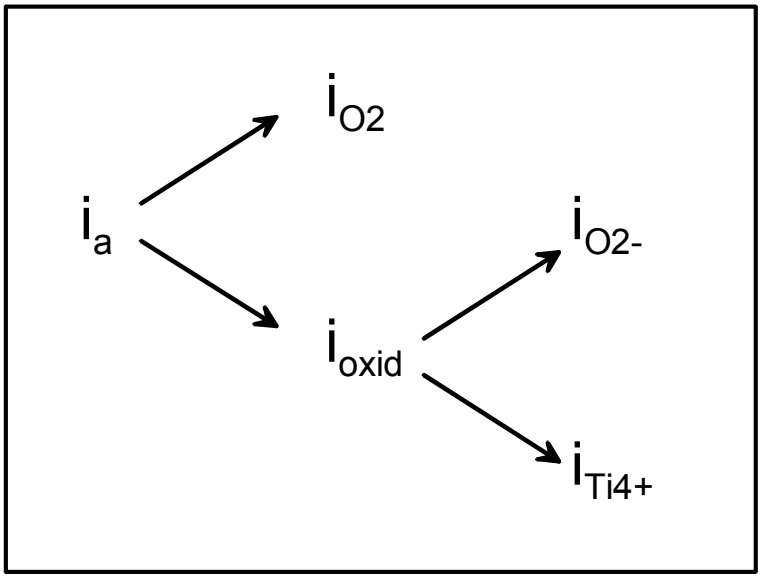

# Oxygen evolution – Where in the oxide layer?

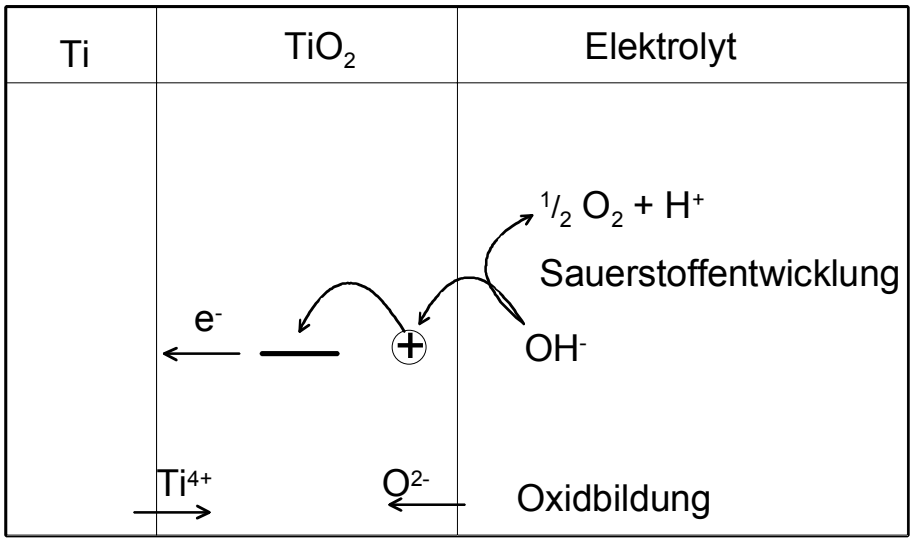


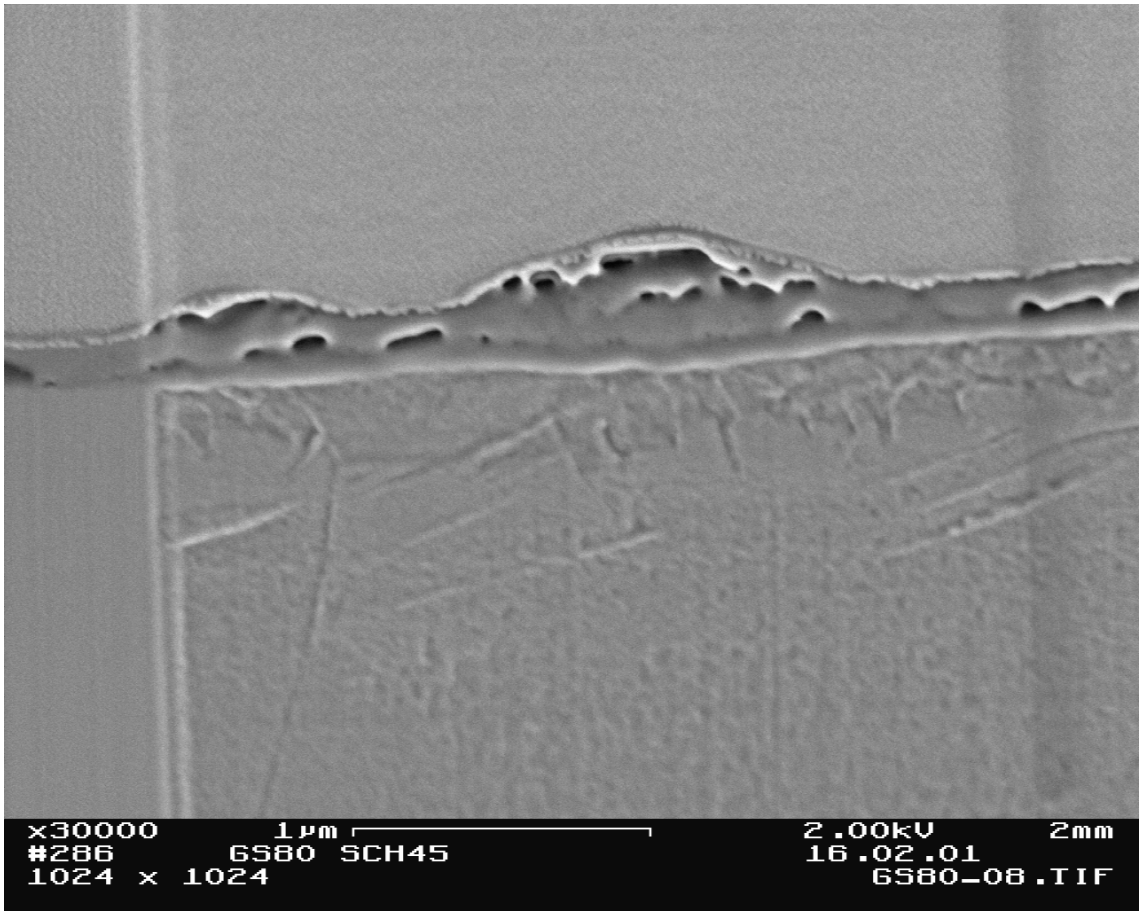


Oxide layer on Ti6Al4V formed with

$i = 6.37\ mA\ cm^{-2}$ to $U = 80\ V_{SCE}$

FIB cross section preparation; (top – platinum bar; middle – porous oxide layer; bottom – Ti6Al4V substrate)

## 8.6. Combinations of metallic biomaterials

Besides pitting corrosion, intergranular corrosion and crevice corrosion, **galvanic corrosion** causes drastic local corrosion, mainly generated by an electron-conducting connection of different materials.

Field of dental surgery - more craftsman-like techniques used in the dental laboratory may cause additional supplementary disadvantageous changes in structure of the materials as result of heat treatment during welding or soldering

Short-circuit potentials and local current investigations of the combining of titanium with several other alloys in a 1 % NaCl solution (pH 6.3), in part with 10 % lactic acid (pH 1.81) showed:

- combination with noble metal alloys: titanium acts as local anode $\rightarrow$ because of stability of the ion-conducting passive layer no increased corrosion takes place
- combination with nickel-based alloys: titanium acts as the local cathode $\rightarrow$ because of the *n*-semiconducting properties of the titanium passive layer increased corrosion appears. Causes corrosion attack of nickel-based alloys + in case of unfavourable surface ratios damage to titanium due to hydrogen embrittlement.

Using different galvanic couples (Ti/gold-based alloys, Ti/palladium-based alloys and Ti/non-precious alloys), titanium was under either cathodic or anodic control.
It has been found, that alloy is potentially useable for superstructures in galvanic coupling with titanium if:

- in a coupling titanium has a weak anodic polarisation
- the galvanic cell current density is also weak
- the crevice corrosion potential is markedly higher than the coupling potential.

# 8.7. Special Materials

Goal: development of alloys being able to replace amalgams

## → Gallium based alloys

(typical) compositions:
solid component: 50 % Ag, 25.7 % Sn, 15 % Cu, 0.3 % Pd
60.1 % Ag, 28.05 % Sn, 11.8 % Cu, 0.05 % Pt
liquid component: 62 % Ga, 25 % In, 13 % Sn, 0.05 % Bi
$F_p$ 10 °C, ($F_p$ for Gallium 29.8 °C

Investigations deoxygenated Ringer's solution at 37 °C showed:

Uncoupled gallium-based alloy at low overpotentials:
selective dissolution of divalent tin ions, followed by a dissolution of Ga

Uncoupled gallium-based alloys and gallium alloy coupled with amalgam: anodic current densities $10^3$-$10^4$ times higher than that of an uncoupled amalgam → very poor corrosion stability.

Comparison of the cytotoxicity of
- gallium and indium ions
- with that of mercuric ions

in a concentration range of 1 µM to 1 mM using L-929 mouse fibroblasts:

mercuric ions:
50 % inhibition at concentration of 0.35 mM
gallium and indium ions:
did not significantly inhibit dehydrogenase activity in either growing or the confluent phase

Effects of metal ions used in dental materials on the conversion of amorphous calcium phosphate to hydroxyapatite *in vitro*:
According to effects on both the rate of hydroxyapatite transformation and induction time:

- inhibitory (in the order: Ni, Sn, Co, Mn, Cu, **Ga**, Th, Mo, Cd, Sb, Mg, **Hg**)
- ineffective (Cs, Ti, Cr, $Fe^{2+}$)
- stimulatory ($Fe^{3+}$, **In**).

## Summary

- similar or better mechanical properties than modern (Hg) amalgams
- difficult manipulation
- low corrosion resistance
- lack of gallium's biological impact

→ restricted use